N89-21738

1988

NASA/ASEE SUMMER FACULTY FELLOWSHIP PROGRAM

MARSHALL SPACE FLIGHT CENTER
THE UNIVERSITY OF ALABAMA

EXPERIMENTAL RESULTS ON ATOMIC OXYGEN CORROSION OF SILVER

Prepared by:	Albert T. Fromhold, Ph.D.
Academic Rank:	Professor
University and Department:	Auburn University Department of Physics
NASA/MSFC: Laboratory: Division: Branch:	 Materials and Processes Engineering Physics Physical Sciences
MSFC Colleague:	Ann F. Whitaker
Date:	August 15, 1988
Contract No.:	NGT 01-002-099 The University of Alabama

EXPERIMENTAL RESULTS ON ATOMIC OXYGEN CORROSION OF SILVER

by

Albert T. Fromhold
Professor of Physics
Auburn University
Auburn University, AL 36849

ABSTRACT

The results of an experimental study of the reaction kinetics of silver with atomic oxygen in 10° increments over the temperature range 0° to 70°C is reported. The silver specimens, of the order of 10,000 Å in thickness, were prepared by thermal evaporation onto 3-inch diameter polished silicon wafers. These were later sliced into pieces having surface areas of the order of 1/4 to 1/2 square inch. Atomic oxygen was generated by a gas discharge in a commercial plasmod asher operating in the megahertz frequency range. The sample temperature within the chamber was controlled by means of a thermoelectric unit. Exposure of the silver specimens to atomic oxygen was incremental, with oxide film thickness measurements being carried out between exposures by means of an automated ellipsometer. For the early growth phase, the data can be described satisfactorily by a logarithmic growth law: The oxide film thickness increases as the logarithm of the exposure time. Furthermore, the oxidation process is thermally activated, the rate increasing with increasing temperature. However, the empirical activation energy parameter deduced from Arrhenius plots is quite low, being of the order of 0.1 eV.

ACKNOWLEDGEMENTS

Acknowledgements are owed to many people, among them the following:

* **Mrs. Ann Whitaker**, MSFC Colleague, for helpful discussions and for use of laboratory equipment, especially the plasma asher and thermoelectric unit

* **Ralph Carruth**, Branch Chief, for his interest and useful suggestions

* **John Reynolds**, for aiding me in establishing communication with the automated ellipsometer

* **Bob DeHaye**, for helpful advice and stimulating ideas

* **David Esker**, Ga. Tech. co-op student, who often lent a hand with the measurements

* **Many other members of the Engineering Physics Division** under the direction of Dr. Ray Gause, for help, advice, and good fellowship

* **Bob Schwinghamer**, Materials and Processes Laboratory Director, for his interest, encouragement, and insightful comments

* **Ron Beshears**, Auburn graduate student, for preparing the evaporated silver specimens

* **Dr. John Williams**, Auburn University Professor, for taking RBS spectra of the oxidized silver specimens

* **Dr. Mike Freeman**, University Program Co-Director, for his generous organizational style and good humor

* **Mrs. Ernestine Cothran**, MSFC Program Co-Director, for her sincere interest and careful attention to detail

I. INTRODUCTION

There is very little atomic oxygen in the ambient atmosphere on earth. That which is produced by decomposition of molecular oxygen by incident ultraviolet radiation from the sun which penetrates the earth's atmosphere undergoes rapid recombination to molecular oxygen because of the high collision rates at atmospheric pressure. The situation is quite different at very high altitudes, where the ultraviolet flux is relatively greater and the pressure is relatively much lower. The molecular oxygen is then decomposed much more rapidly, and the recombination rate due to atomic collision is vastly reduced. The primary form for oxygen at altitudes of low earth orbit trajectories is therefore atomic. One might initially think that the low ambient pressure at low earth orbit trajectories would imply little gas-solid interaction, but this is not true. The interaction of atomic oxygen with various materials has important implications for NASA's space telescope and space station programs.

The basic problem is that atomic oxygen is so much more reactive than molecular oxygen that corrosion effects on materials are greatly worsened in low-earth orbit, relative to corresponding rates on earth. One of the best examples of this is the deterioration of the elemental metal silver while exposed on board the space shuttle (1,2). Silver is swiftly attacked by atomic oxygen to form a black oxide layer which subsequently cracks and spalls. The purpose of the presently-described experimental work was to study the very early stages of the oxidation of silver by atomic oxygen.

The Physical Sciences Branch of the Engineering Physics Division of the Materials and Processes Laboratory of Marshall Space Flight Center has a renowned history in studying atomic oxygen effects on various materials, including elemental metals, alloys, organics, epoxy resins, paints, *etc.* The laboratory personnel have carried out flight experiments, supplemented by many ground-based experimental studies (1,2). The measurements described herein were carried out in collaboration with the members of that laboratory using their facilities.

II. OBJECTIVES

The primary objective of this study was to determine experimentally the early-stage kinetics of the reaction of atomic oxygen with silver. This requires determination of the oxide film thickness as a function of exposure time at a given temperature, with a series of temperatures employed to determine the temperature dependence of the kinetics. The secondary objective was to explore the theoretical implications of the experimental results.

III. EXPERIMENTAL

A. Procedures

Polished silicon wafers were used as substrates for evaporated silver layers 10,000 Å in thickness, as measured by a Dektak mechanical profiler. After evaporation, the wafers were cut into smaller specimens 1/4 to 1/2 inch on edge. Before each temperature run, the optical constants of the silver specimen were measured with a Gaertner automated ellipsometer having a laser (λ = 6328 Å) light source for producing the measuring beam. Typical values for the refractive index and absorption coefficient were $n_s = 0.1$, $k_s = 3.8$. Reaction with atomic oxygen produced a surface oxide having typical optical constant values of $n_f = 1.8$, $k_f = 0.1$, though a range of values [$(1.6 \leq n_f \leq 2.2)$; $(0.05 \leq k_f \leq 0.25)$] for each was required to satisfy the minimum error criterion for different thicknesses.

Specimens were placed in the chamber of a commercial plasma asher which was pretuned at the operating conditions of 60 Watts and 800 millitorr oxygen pressure. The flux of atomic oxygen under these conditions has been estimated (3) to be $10^{18}/cm^2$-sec. After locating the specimen on the thermoelectric temperature controller in the chamber, evacuation was carried out by a vacuum pump operating with a nonorganic fluid, and the temperature of the specimen was regulated by adjusting the voltage on the thermoelectric device. A constant-temperature chilled solution was circulated continuously through the mounting block for the thermoelectric device and specimen in order to provide the reference temperature and a heat source and sink. The sample temperature was monitored with a thermocouple. Oxygen pressure was varied by adjusting the rate of steady-state flow of molecular oxygen into the chamber. After achieving the desired temperature, the oxygen pressure was raised and stabilized at 800 millitorr, and the gas discharge initiated. Initial specimen exposures were in half-second increments, but the length of the exposure increment was steadily increased as the reaction rate decreased. Initial exposure periods were required to be this short because of the very high initial reaction rates. However, there is definitely some uncertainty in the timing of such extremely short bursts of the gaseous discharge. After each exposure, the specimen was allowed to return to ambient temperature in the reaction chamber. It was then removed from the chamber, placed in air on the stage of the automated ellipsometer, and the surface oxide film thickness measured. For reasons which become apparent in the next section, especial care was taken to shutter the laser light to prevent exposure of the sample except during the short time increment (20 seconds or so) required for the ellipsometer to collect the optical data needed for computation of the oxide thickness in a given measurement. Following determination of the thickness, the sample was returned to the plasmod reaction chamber, and the cycle repeated.

B. Interaction of Laser Beam and the Oxide Film

An unexpected interaction was found between the laser light beam of the ellipsometer used for oxide film thickness measurement and the oxide film itself, namely, the readings of the ellipsometer for the film thickness were found to change slowly but continuously if the light beam was reflected continuously from the sample during and between individual measurements. This effect is shown in the bar graph for oxide film thickness in Fig. 1, where it can be noted that the thickness reading continuously decreases with the measurement number while the light is continuously reflected from spot A on the specimen. Moving the sample stage so that the light is reflected from a new position (spot B) yields initially a higher thickness reading, but that reading then also continuously decreases with the measurement number.

Such an interaction between observer (measuring instrument) and the object (that which is observed) is expected on a microscopic level, being the raison d'être of the Heisenberg uncertainty relation. However, it was surprising to us to find the effect on such a macroscopic level. This is perhaps indicative of the relative instability of silver oxide, especially under the uncontrolled ambient conditions in air while the sample was on the ellipsometer stage during measurement. It could even be associated with changing optical properties of the oxide because of continuous exposure to the light beam. Irrespective of the nature of the observed effect, our practical solution to this problem was quite straightforward -- we simply shuttered the light beam from the sample being measured except for the brief period required for the ellipsometer to collect the data in each measurement.

C. Oxidation Kinetics

Figure 2 illustrates the increase in oxide film thickness with time of exposure to atomic oxygen for a silver specimen held at a temperature of 20°C during exposure. Note from this figure that the oxide thickness initially increases very rapidly with exposure time, but this is followed by a leveling off to a slow growth region. The observed behavior was found to be typical of the data taken at all temperatures utilized in this study, namely, 0, 10, 20, 30, 40, 50, 60, and 70°C. Not all data, however, were taken over such an extended exposure period as that for the data in Fig. 2, which can be noted to extend out to a cumulative value of 280 seconds. The maximum oxide film thickness obtained for this exposure can be noted to be of the order of 2600 Å.

Corresponding data taken at a temperature of 40°C are shown in Fig. 3. This curve exhibits also the initial rapid growth phase, followed by the leveling off to a much slower growth period. The maximum exposure time for the 40° data can be noted to be 26 seconds, at which time the oxide film thickness can be noted to be approximately 2000 Å.

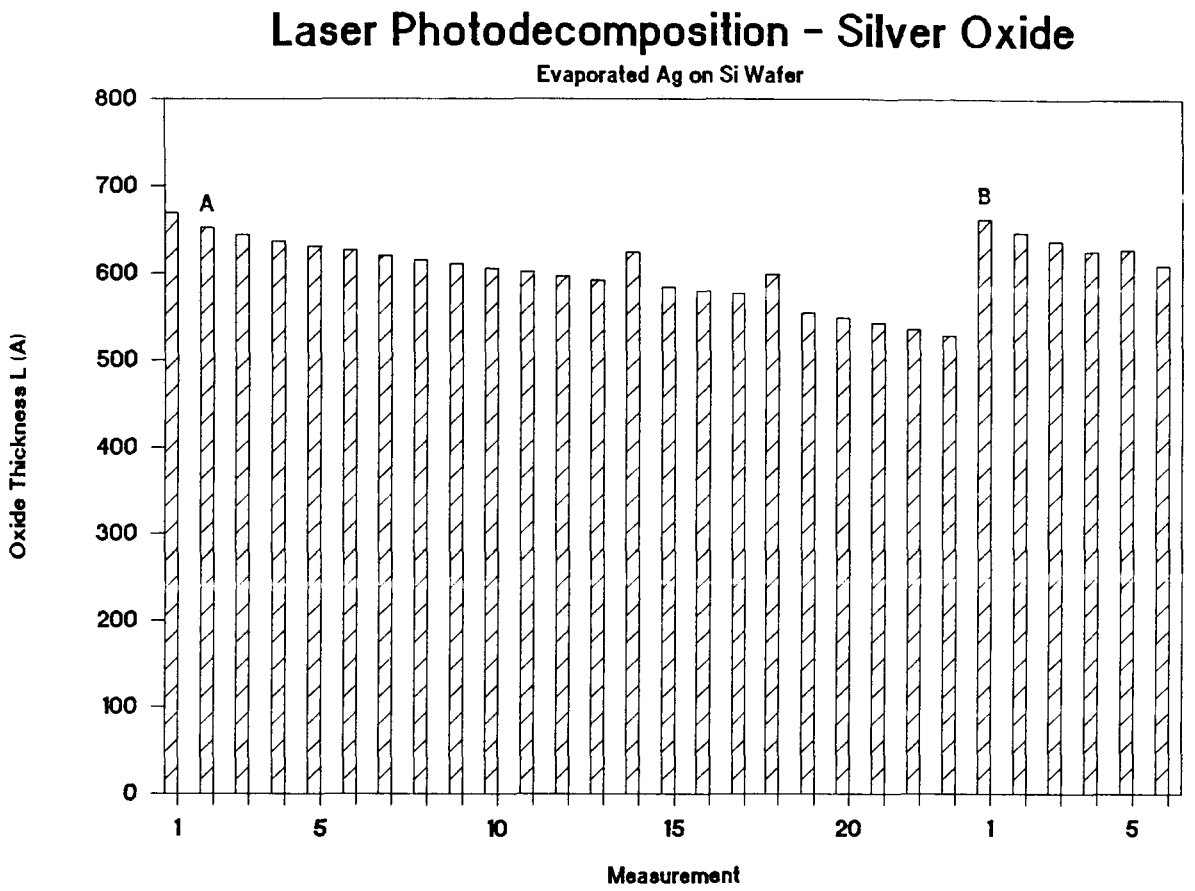

Figure 1 - Curious Heisenberg uncertainty interaction of the measurement beam of the ellipsometer with the measured oxide film.

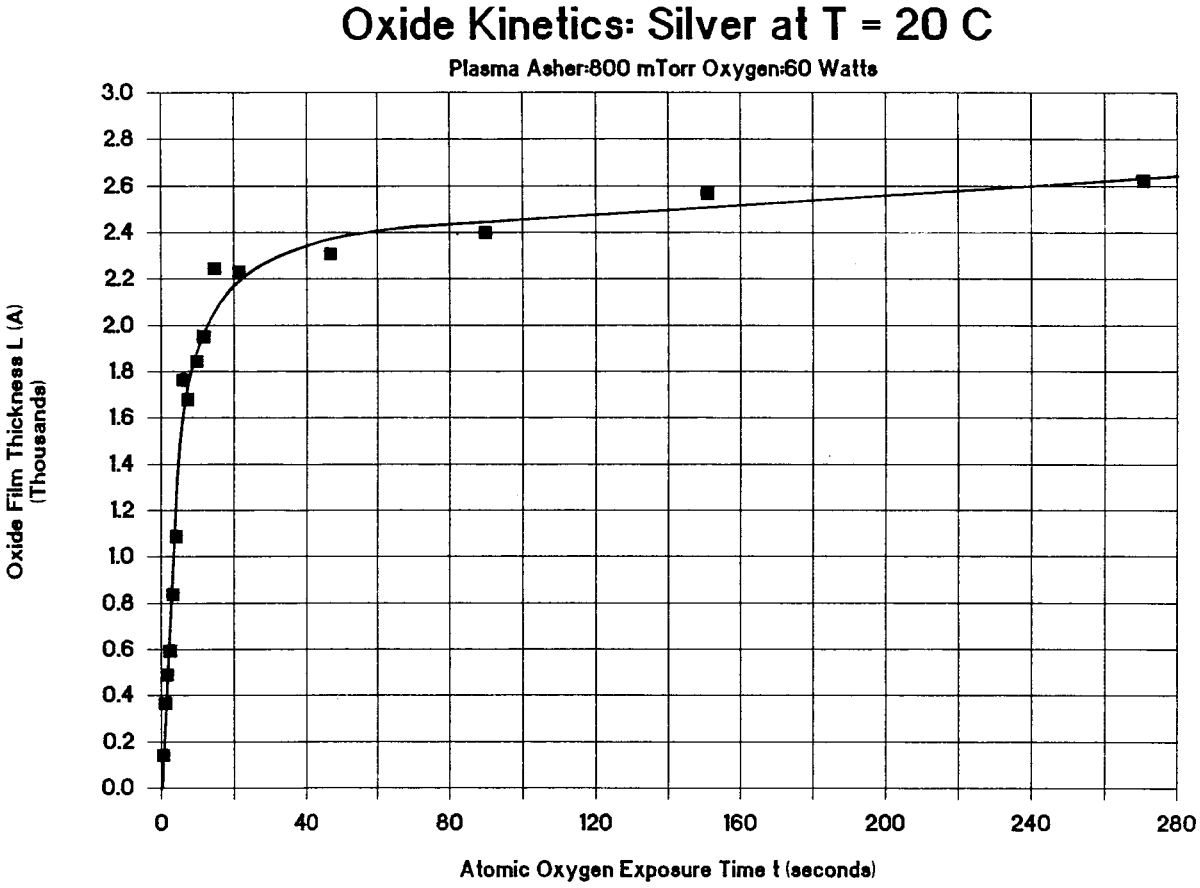

Figure 2 - Linear plot of the oxide film thickness versus exposure time for a temperature of 20 C.

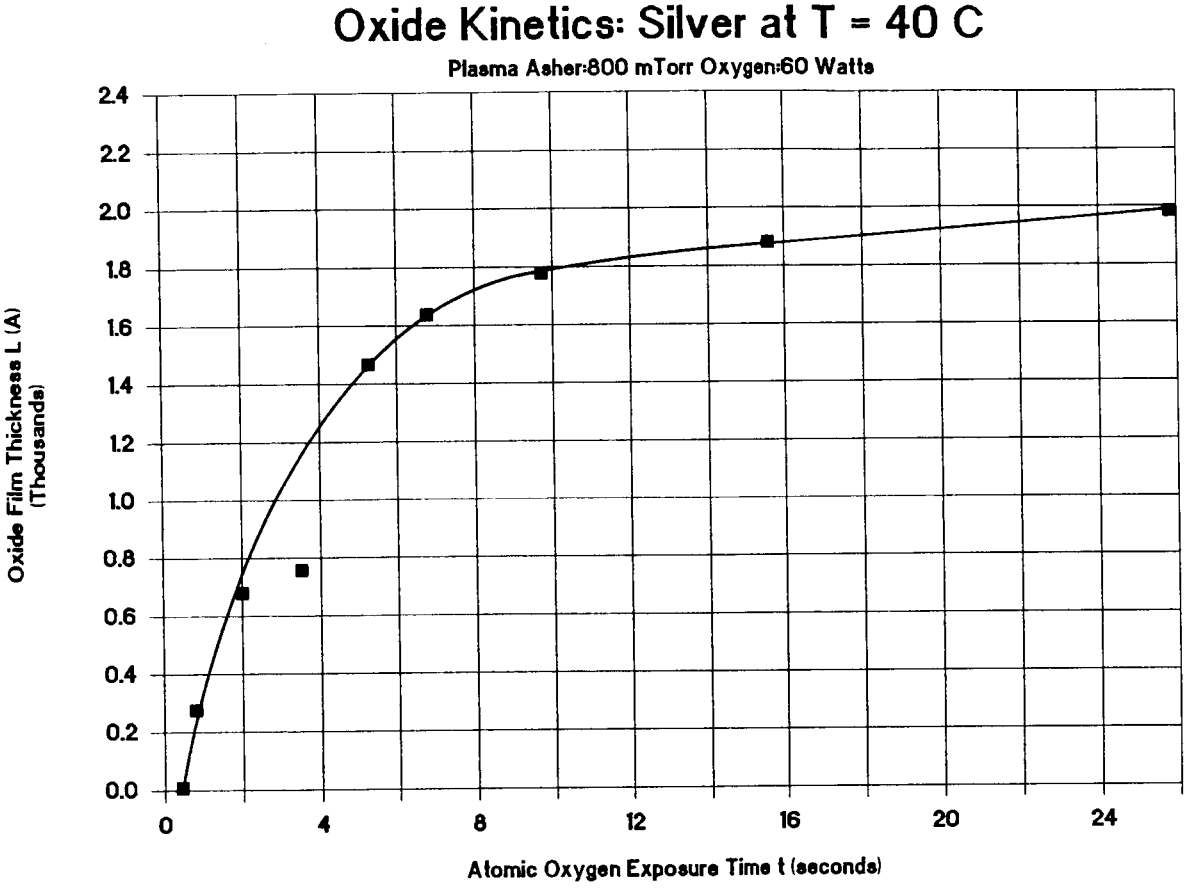

Figure 3 - Linear plot of the oxide film thickness versus exposure time for a temperature of 40 C.

Figure 4 illustrating corresponding data taken at 60°C also exhibits the same behavior typical of Figs. 2 and 3, namely a fast growth period followed by a slow growth period. For an exposure of 45 seconds, the oxide thickness achieved can be noted to be approximately 2100 Å.

Data taken at the other temperatures of this study were found to exhibit the same general trends illustrated by Figs. 2-4. These data are not specifically shown herein, but the results are used in our analysis. There was a general trend for the thickness at an arbitrary exposure time to increase with increasing temperature, indicating a thermally-activated oxide growth process.

D. Related Observations

Examination of the oxidized surface under a low power microscope showed that black islands form and increase in size in the later stages of exposure. Furthermore, a point is finally reached after extensive exposure to the atomic oxygen where the integrity of the oxide film is destroyed. At that point, the surface of the oxide when observed visually appeared to be flakey. These observations are particularly relevant to the lack of protectiveness of silver oxide for the underlying silver under attack by atomic oxygen. It may be stated that even though the growth kinetics observed for the early stages of oxidation in this study would seem to imply that the oxide layer being formed represents a highly protective barrier layer in preventing continued reaction of oxygen and silver, as reflected in the slow growth rate found in the later stage of growth, this is a bit misleading because this phase of oxidation is followed by a second phase of the reaction which is very deleterious to the coherence of the layer.

Lack of uniqueness in interpreting ellipsometer readings for nonhomogeneous oxide films makes it advisable to complement those results with data obtained by other techniques. The most direct method we used to verify that the thickness of the oxidized silver is increased over that of the pure silver was to trace the diamond stylus of a mechanical surface profiler from the bare silicon wafer onto the surface of the silver layer before reaction and after reaction. The increase in volume produced by oxidation of silver is a factor of approximately 1.5, so the oxidized silver is thicker. A third experimental probe which we used to examine some of our oxidized specimens was that of Rutherford backscattering, *viz.*, **RBS**. The spectra were generally consistent with the ellipsometer deductions.

A good indication that the oxide film constitutes a separate phase on the surface of the silver was given by the interference colors observed on the silver specimens after various times of exposure to the atomic oxygen. Light gold was followed by a deeper gold, subsequently followed by violet and then blue. Oxidizing further gave a silver color, followed by second-order interference colors beginning with light gold.

IV. ANALYSIS

A. Growth Law

The most commonly-observed thermally activated oxide film growth law (4,5) is that in which the film thickness increases as the square root of the exposure time. This is known as the **parabolic growth law**. Theoretically such a law follows, for example, from the application of Fick's laws of diffusion to the steady-state transport of uncharged point defect species of oxygen or metal atoms moving through the barrier represented by the existing oxide film. Once the diffusing species reach the other side of the oxide film, the chemical reaction of new oxide formation can occur, and the oxide film is increased in thickness. The parabolic law also holds under similar conditions whenever the moving point defect species are charged. Therefore the theoretical base is strong for a parabolic growth law of some type, in which case

$$L(t) \propto t^{1/2} , \qquad (1)$$

where L(t) is the oxide thickness at time t. The proportionality constant appropriate for this relation would depend upon the specifics of the experimental parameters and the metal, the state of charge of the mobile point defect species, the mobilities and boundary concentrations of the species involved, and the amount of space charge in the oxide due to these mobile species (4,5). Independent of the actual value of the proportionality constant, however, plots of the oxide film thickness versus the square root of the exposure time would be straight lines if any type of parabolic growth law is applicable, irrespective of the specific value of the rate constant.

To test whether our experimental data conform to a parabolic growth law, we made plots at each temperature of the oxide thickness versus the square root of the exposure time. One example of these plots is shown in Fig. 5, where the Fig. 4 data taken at 60°C are replotted in parabolic form. It is clear from a cursory inspection of Fig. 5 that a straight-line relation is not obtained for the data by such a plot, so that a parabolic growth law is definitely not appropriate for describing our data. The parabolic plots for the data taken at other temperatures in this experimental study likewise gave no support for the applicability of the parabolic growth law.

An alternate growth law sometimes found to fit empirically some experimental oxide growth rate data is the cubic growth law, for which the oxide film thickness increases as the cube root of the time,

$$L(t) \propto t^{1/3} . \qquad (2)$$

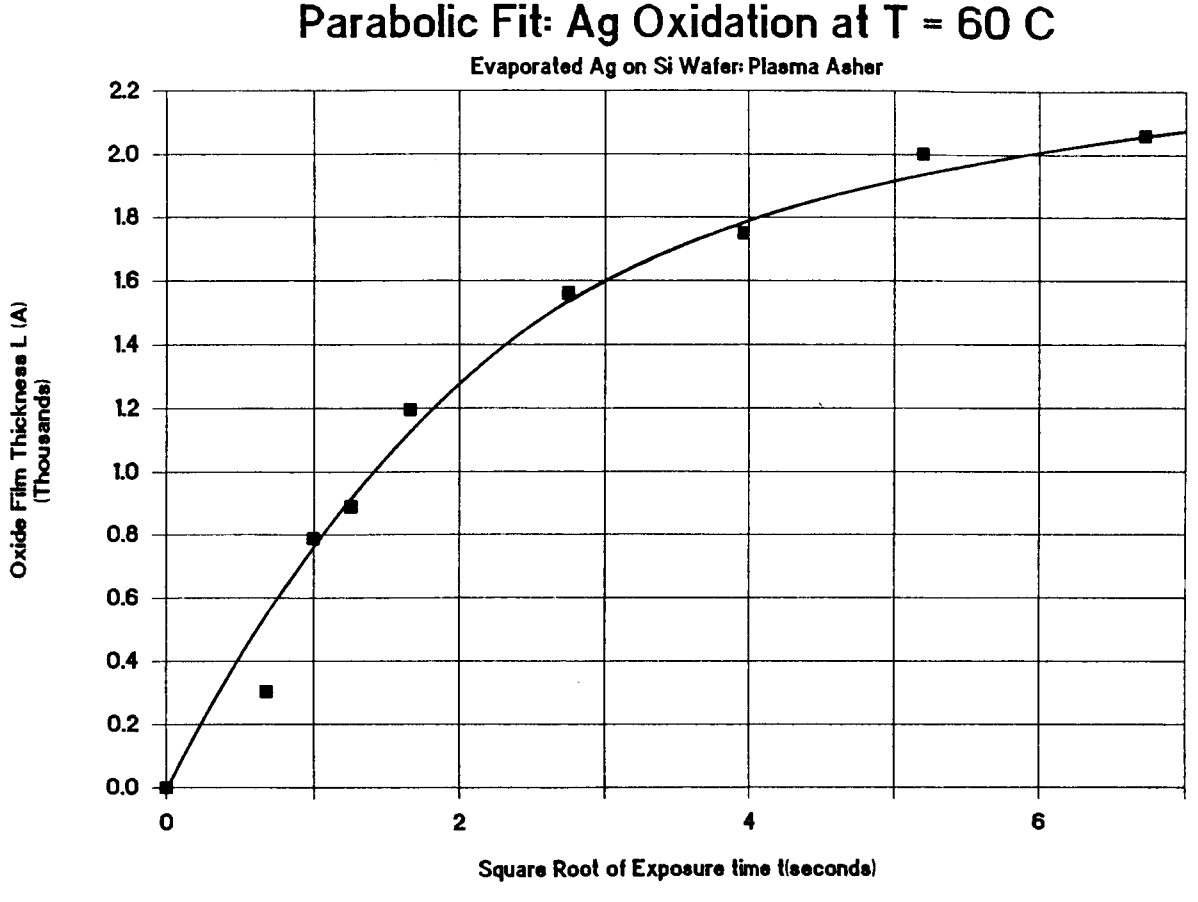

Figure 5 - Parabolic plot of the oxide film thickness versus exposure time for a temperature of 60 C.

To explore this possibility, we made plots of the thickness as a function of the cube root of the time for our data at each of the temperatures of this study. Figure 6 shows the plot for the 60°C data. It is evident that a straight-line relation does not describe well the experimental data plotted in this manner. The corresponding plots at the other temperatures of this study likewise did not obey straight-line relationships, so the conclusion was reached that our data do not conform to a cubic growth law.

The empirical logarithmic growth law

$$L(t) \propto \log t \qquad (3)$$

is sometimes found to be useful for fitting experimental oxidation data. Because our data failed to conform to both the theoretically well-based parabolic growth law and the more empirical cubic growth law, the next step was to try semilogarithmic plots of the data to see if the empirical logarithmic law could provide a framework for describing the data.

Figure 7 shows the results of fitting a straight line to the oxide film thickness data at 60°C (*cf.* Fig. 4) after replotting as a function of the logarithm (to the base 10) of the exposure time. Although the straight line drawn through the data points in Fig. 7 is not by any means in perfect agreement with all of the data, it nevertheless provides an acceptable fit in the sense of giving the proper general trend. Such plots were also constructed for the data taken at the other temperatures of this study. For example, Fig. 8 shows the semilogarithmic plot of the 40°C data. Again the fit of the straight line to the kinetics data is acceptable. Since this conformity was also found for the data at the other temperatures, we concluded that the logarithmic growth law provides an acceptable description of our kinetic studies on the oxidation of silver by atomic oxygen over the temperature range 0 to 70°C.

B. Logarithmic Growth Law Parameters

The general equation for a straight line, namely $y(x)=mx+b$, where the dependent variable y changes linearly with the independent variable x, yields a line having slope m and y-intercept b. Our analog of this relation is

$$L(t) = L_{crit} \log_{10} t + b_0 \ , \qquad (4)$$

where L(t) is the oxide film thickness after the accumulated exposure time t, with the parameters L_{crit} and b_0 representing the slope and the intercept, respectively. Equation (4) was fit to our data at the various temperatures. A pictorial representation of the deduced values for the slope L_{crit} at each temperature is shown in the bar graph of Fig. 9, while the deduced value of the intercept b_0 at each of the

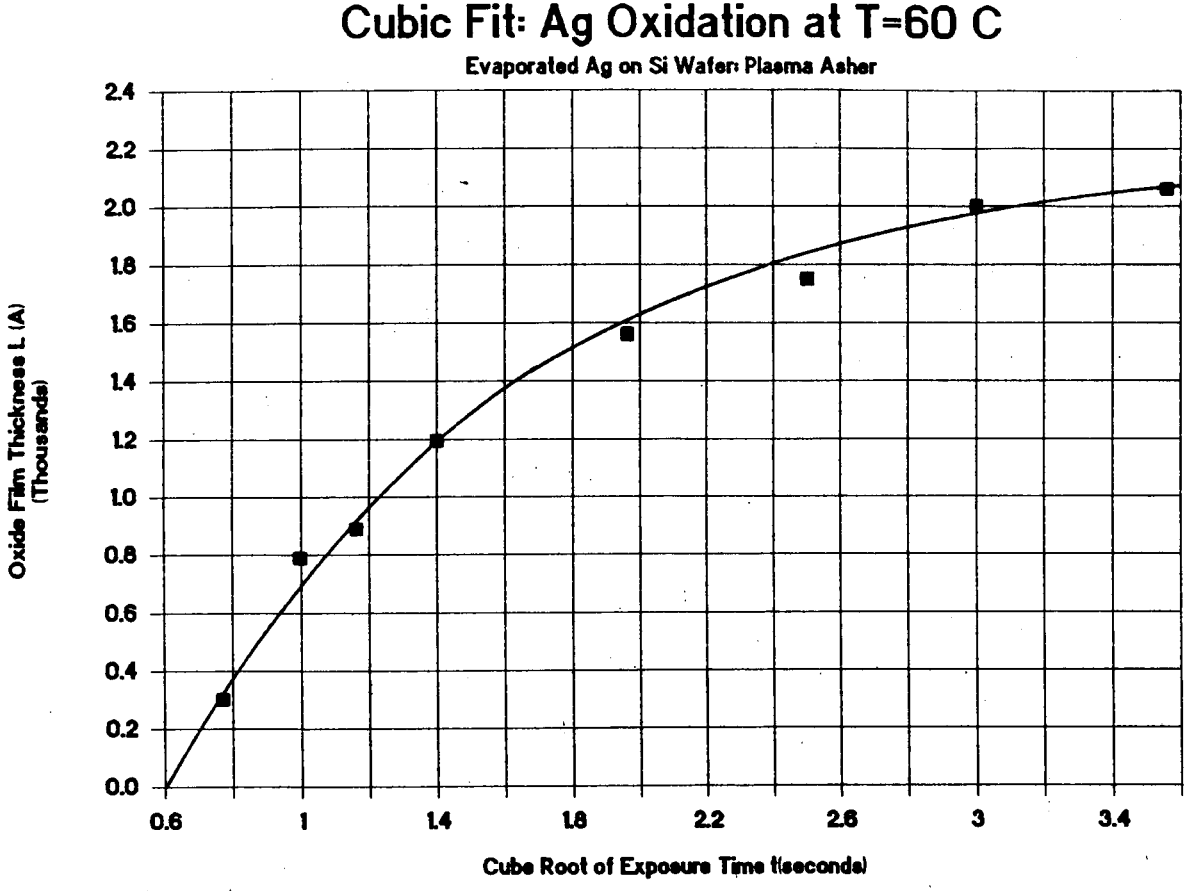

Figure 6 - Cubic plot of the oxide film thickness versus exposure time for a temperature of 60 C.

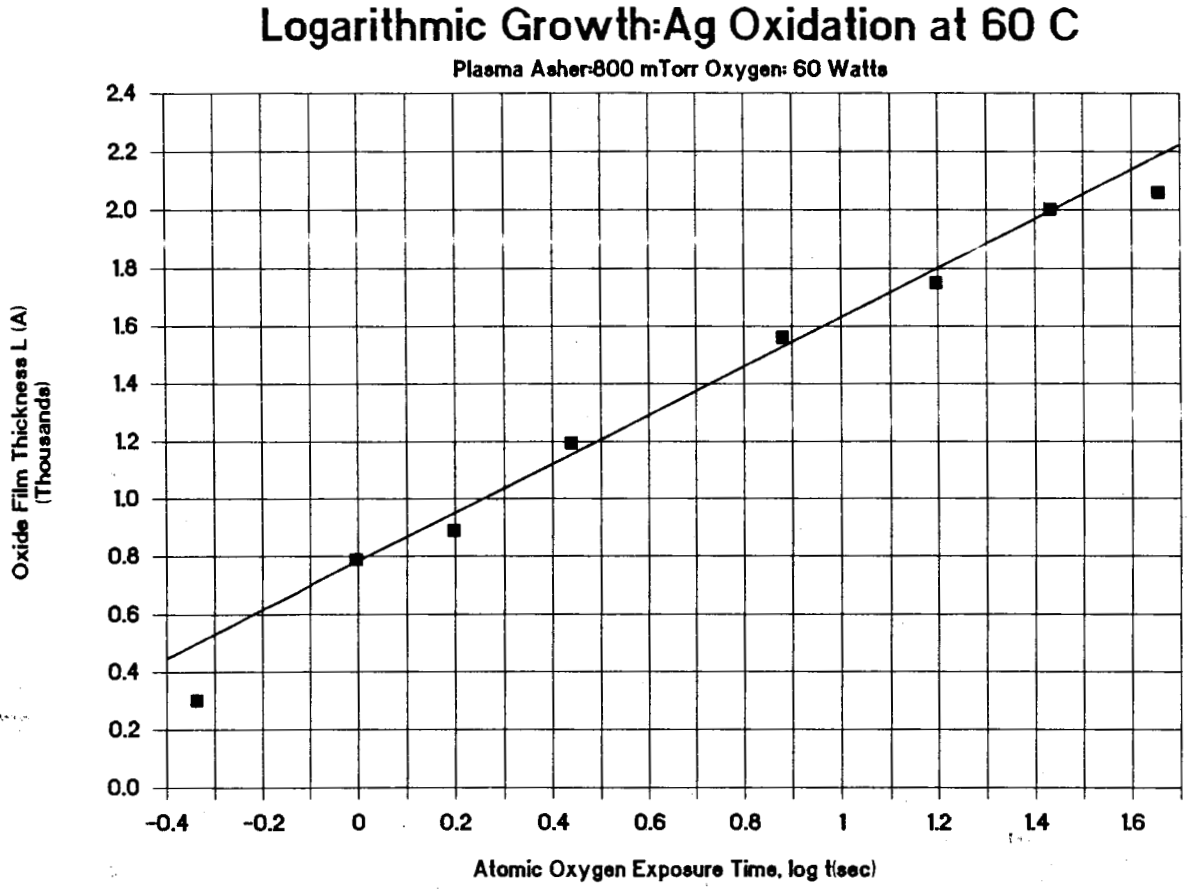

Figure 7 - Semilogarithmic plot of the oxide film thickness versus exposure time for a temperature of 60 C.

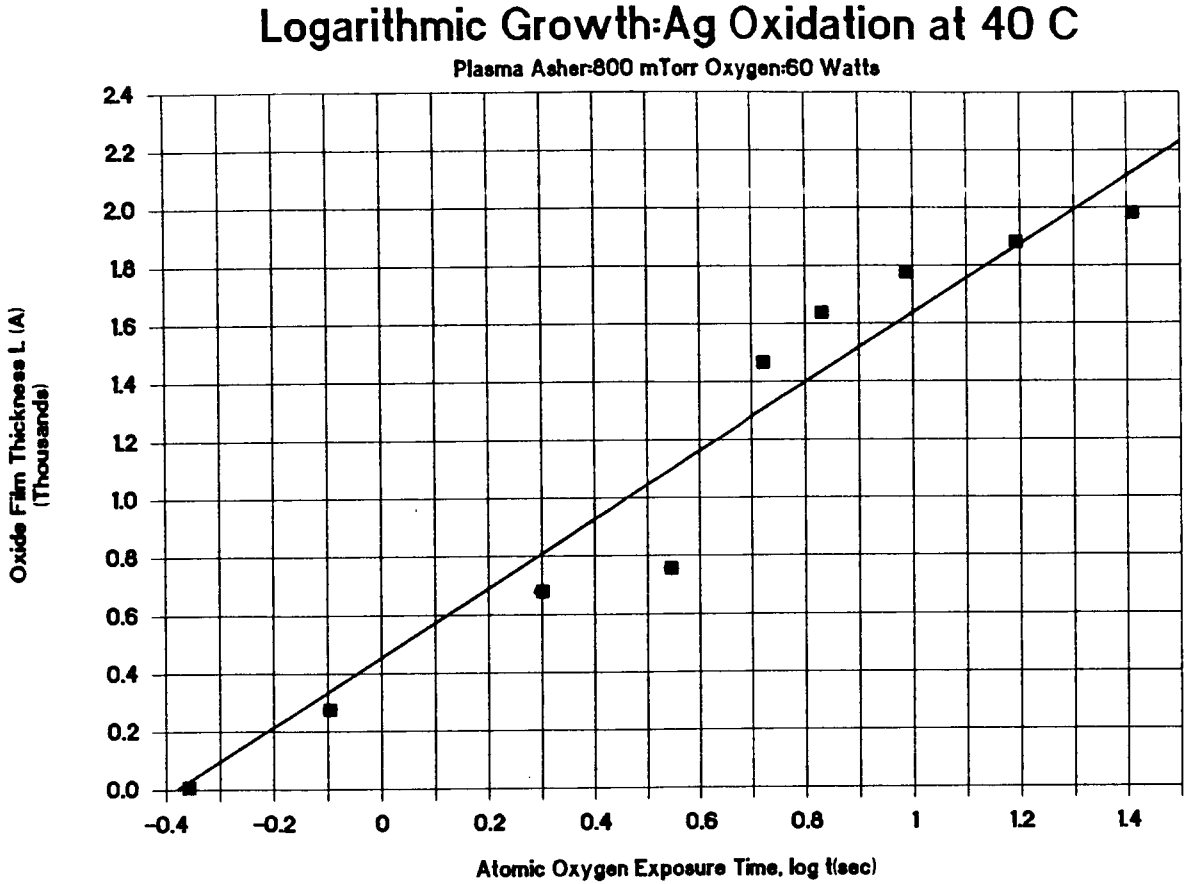

Figure 8 - Semilogarithmic plot of the oxide film thickness versus exposure time for a temperature of 40 C.

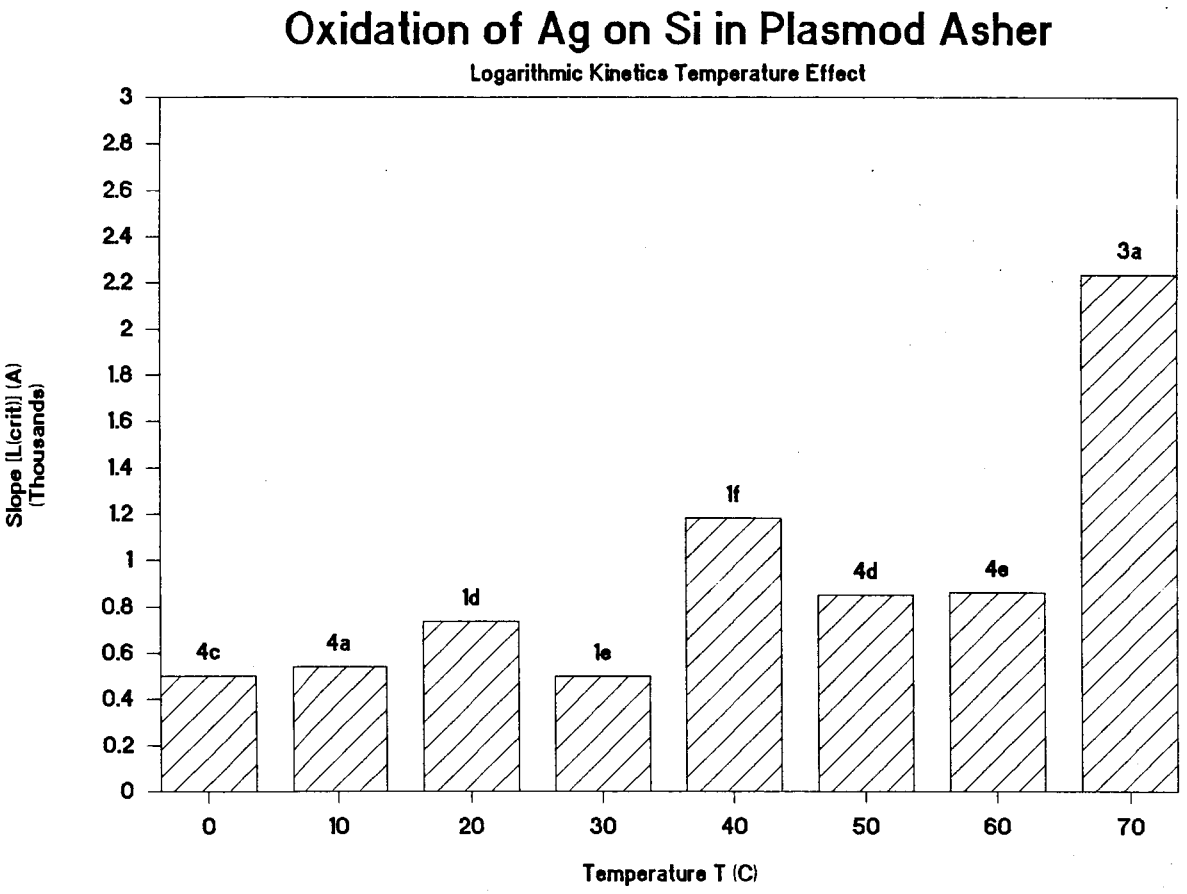

Figure 9 - Temperature variation of the slope of the logarithmic plot of the kinetics.

temperatures is shown in the bar graph of Fig. 10. Note the tendency for both L_{crit} and b_0 to increase with increasing temperature.

Without adopting a specific microscopic model yielding a theoretically well-founded logarithmic growth law, it is not possible to predict the temperature-dependence of the parameters L_{crit} and b_0 which appear in Eq. (4). However the experimental trend is for these parameters to increase with increasing temperature, as noted in the bar graphs of Figs. 9 and 10. This suggests constructing Arrhenius plots for these parameters.

An Arrhenius plot for a thermally-activated quantity Z(T) yields a straight-line relation when the natural logarithm ln[Z(T)] is plotted as a function of the reciprocal of the absolute temperature T. For our parameters L_{crit} and b_0, this would correspond to the functional dependences

(5) $L_{crit} \propto \exp(-U_C/k_BT)$,

(6) $b_0 \propto \exp(-U_B/k_BT)$,

where k_B is the Boltzmann constant and U_C and U_B are parameters having units of energy. The parameters U_C and U_B are related in some presently unspecified way to the activation energy U_{act} for the reaction. The relationship may be half the activation energy U_{act}, or some other function of U_{act}, depending upon the particular microscopic theory underlying the logarithmic law [Eq. (4)] for this particular experimental system.

Plots were constructed for $\ln(L_{crit})$ versus $1/k_BT$ and for $\ln(b_0)$ versus $1/k_BT$, using our deduced values for L_{crit} and b_0. The results of these plots are shown respectively in Figs. 11 and 12. The straight line fits to the data obtained in this manner, although not impressive in quality because of the relatively large scatter in the deduced parameters at the various temperatures, nonetheless provide reasonable descriptions of the trends indicated by the data. The slopes of these lines yield the following energy values:

$$U_C = 0.110 \text{ eV},$$

$$U_B = 0.137 \text{ eV}.$$

The precision of these values is certainly no better than 50%. If one wishes to be more conservative, taking into account the rather limited temperature range studied, the uncertainty in the cumulative exposure times due to the extremely short incremental exposure periods, and the relatively large scatter in the experimental data, then one should probably not claim the precision to be better than a factor of 2.

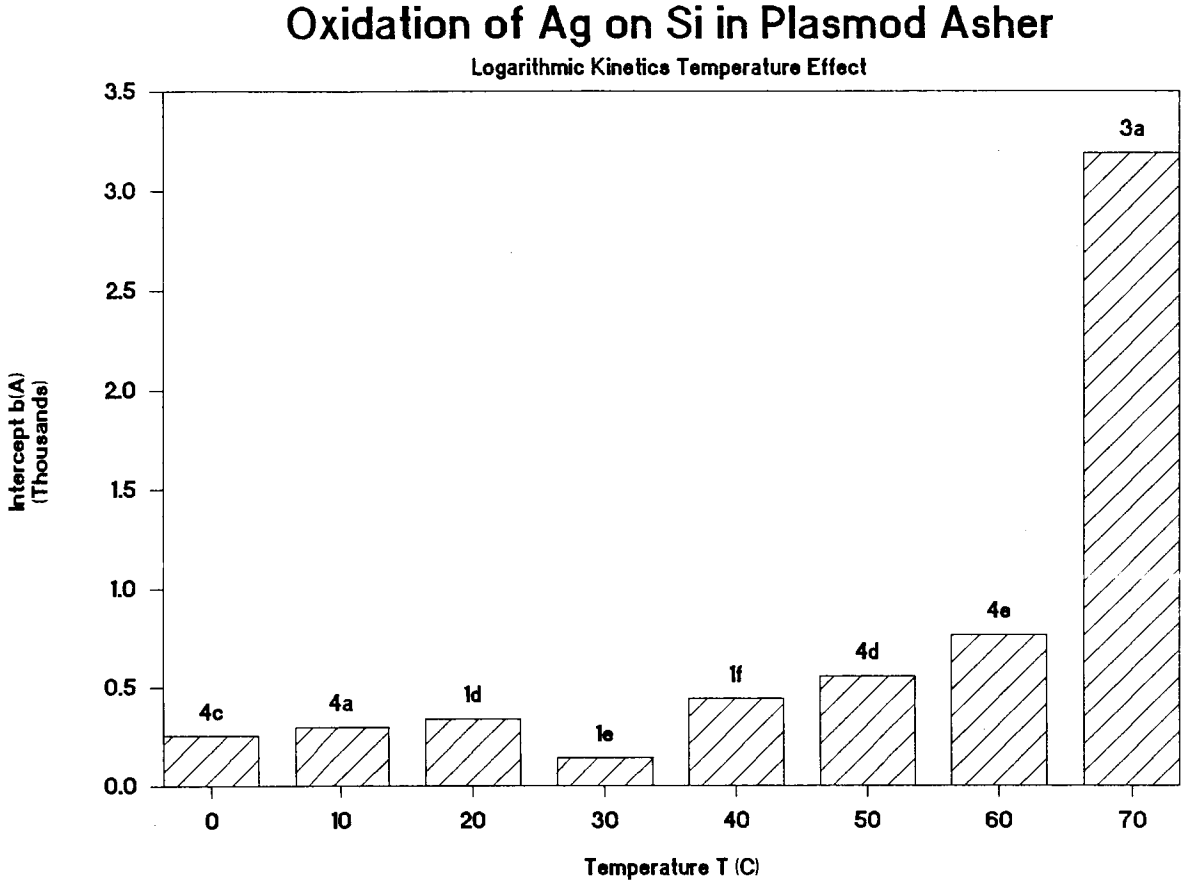

Figure 10 - Temperature variation of the intercept of the logarithmic plot of the kinetics.

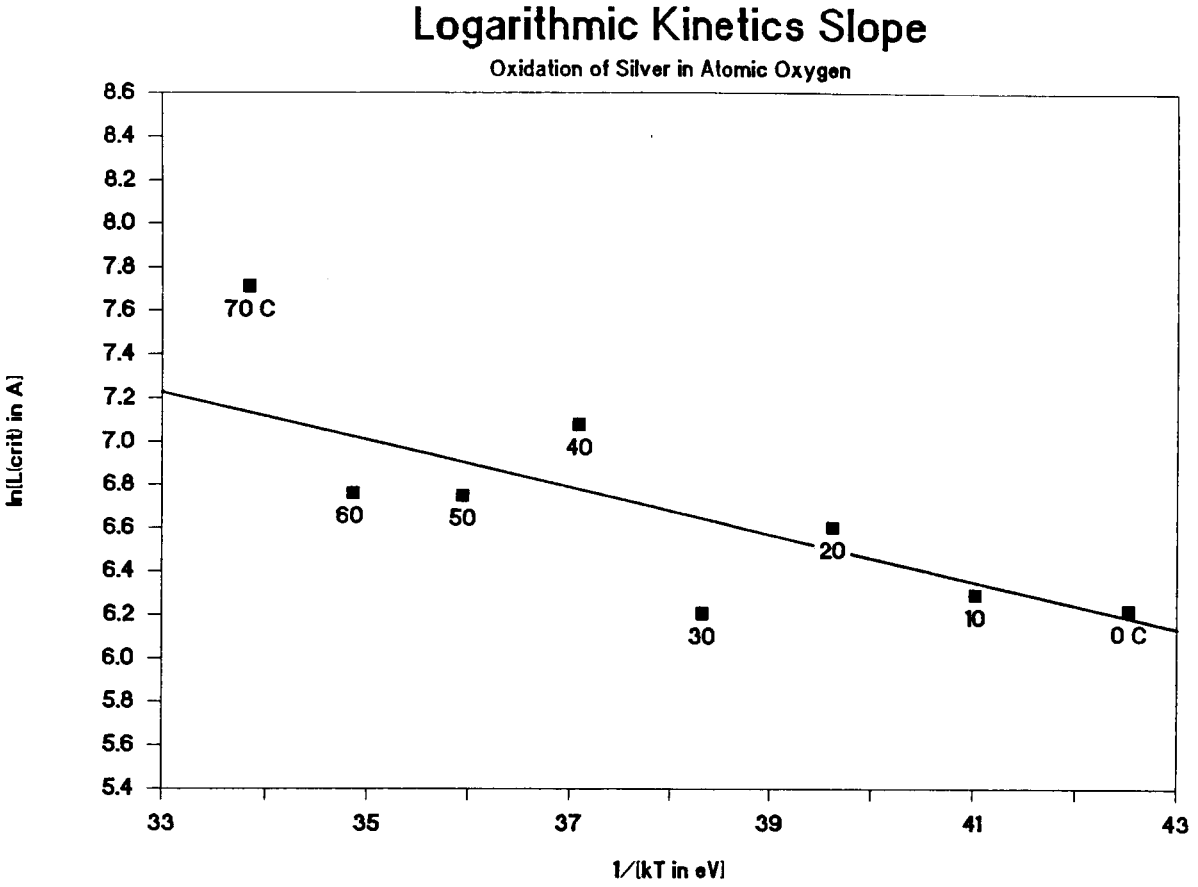

Figure 11 - Arrhenius plot of the slope for the logarithmic kinetics.

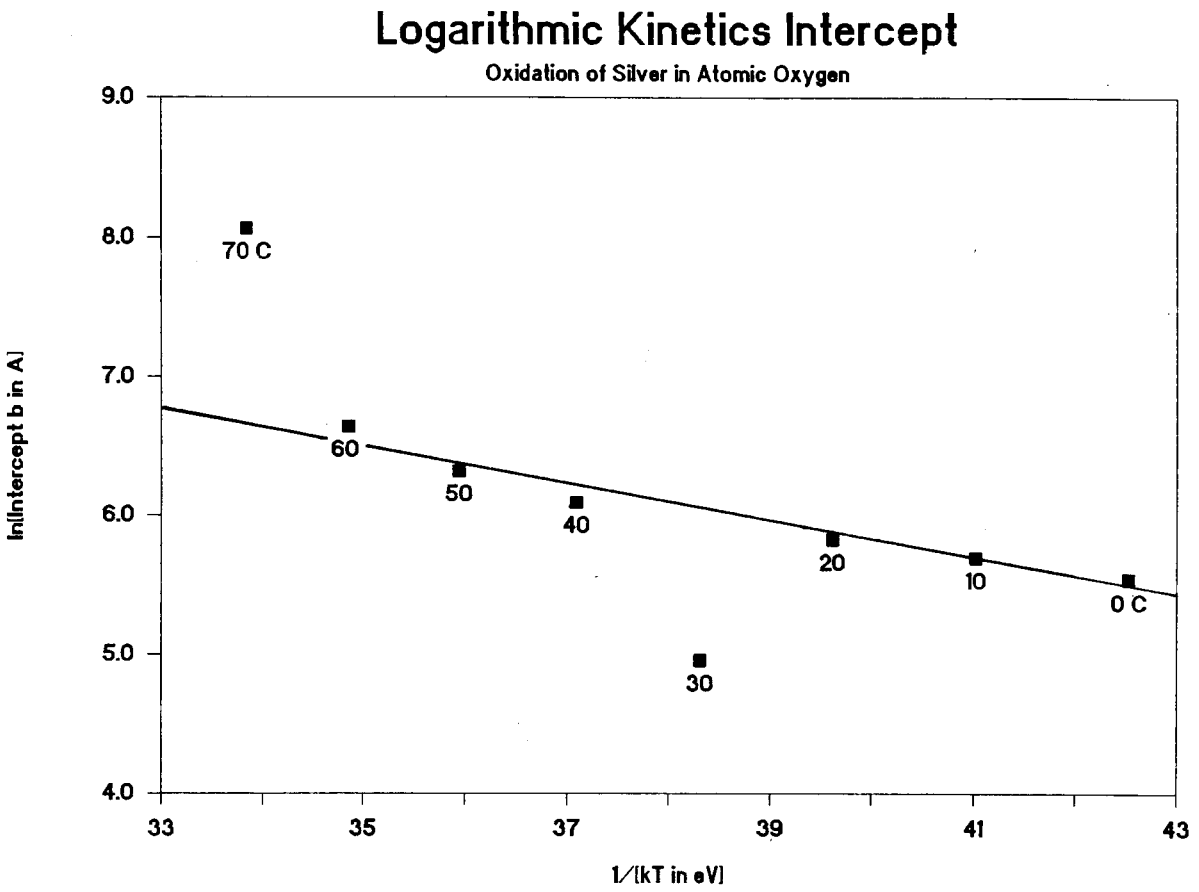

Figure 12 - Arrhenius plot of the intercept for the logarithmic kinetics.

V. CONCLUSIONS

1. Early stage oxidation of silver in atomic oxygen occurs in accordance with the logarithmic growth law.

2. The oxidation is thermally activated, the rate increasing somewhat with increasing temperature.

3. There is an interesting interaction of the laser beam with the oxide.

VI. RECOMMENDATIONS

My first recommendation is to design and construct a reaction chamber which would fit directly in the ellipsometer so that measurements could be carried out continuously *in situ*. This would eliminate a measure of uncertainty introduced by truncating the exposure periodically to carry out measurements of the oxide film thickness with the ellipsometer. Next, discharge conditions (power and oxygen pressure) should be sought which lead to a much slower reaction rate than that encountered in the present experimental study. The reason for this is that continuous exposure under the present experimental conditions would lead to growth rates which could not be followed by the automated ellipsometer even using the instrument in its most optimum fast mode. Then software should be developed to compute the oxide film thicknesses *off-line* after the measurements are complete because the process of varying optical constants until good convergence is attained *on-line* would be impossible if the film were itself changing rapidly during measurement.

A different type of recommendation is to extend the present study to bulk silver specimens to see how the results are affected by the additional roughness and different texture of mechanically-polished surfaces, relative to smooth evaporated surfaces. The refractive index of evaporated silver is about 0.1, while that of mechanically-polished bulk silver surfaces is frequently found to be in the range 0.3 to 0.6.

The effects of grain boundaries on the silver reaction with atomic oxygen are also of great interest. A comparison of data taken on single crystals, which have no grain boundaries, with corresponding data taken on bulk samples, would thus be valuable. At present it is not known to what extent the atomic oxygen diffuses into silver by bulk diffusion and to what extent the diffusion is enhanced by the presence of grain boundaries.

More attention should also be given to theoretical aspects. Assuming that the early-stage logarithmic growth law deduced in this study is confirmed by more precise and extensive experiments carried out over a wider temperature range, then it would be of great interest to seek the basic mechanism which explains such growth. In addition, the effects of mechanical stress should be included in the theoretical formulation.

Finally, these studies should be extended to other metals. It would be relatively easy, for example, to duplicate this series of experiments for evaporated films of aluminum, copper, nickel, and gold. In addition, measurements should be made on elemental metals and alloys which are potentially important for the forthcoming space station.

REFERENCES

1. A. F. Whitaker, S. A. Little, R. J. Harwell, D. B. Griner, R. F. DeHaye, and A. T. Fromhold, Jr., "Orbital Atomic Oxygen Effects on Thermal Control and Optical Materials -- STS-8 Results", AIAA-85-0416, AIAA 23*rd* Aerospace Sciences Meeting, January 14-17, 1985, Reno, Nevada.

2. Albert T. Fromhold, Jr., Ann F. Whitaker, Kasra Daneshvar, and Sally A. Little, "Reaction of Metals in Lower Earth Orbit during Space Shuttle Flight 41-G (STS-17)", AIAA-86 Aerospace Sciences Meeting held in Houston, Texas, November, 1986.

3. A. F. Whitaker, private communication, July, 1988.

4. A. T. Fromhold, Jr., **Theory of Metal Oxidation. Vol. I -- Fundamentals** (North Holland Publishing Company, Amsterdam, 1976), pp. 104, 135, 146.

5. A. T. Fromhold, Jr., **Theory of Metal Oxidation. Vol. II -- Space Charge** (North Holland Publishing Company, Amsterdam, 1980), pp. 178-179, 188.